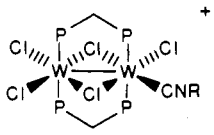

3 (R = mes, xyl, t-Bu)

Accordingly, species of this type can be viewed as substitution derivatives of **2**. The $^{31}P\{^1H\}$ resonances are broad and are shifted upfield from free dppm (δ -22.7).

The electrochemical properties of **3a-c** were studied by cyclic voltammetry (see Figure 1c). Data for solutions in 0.1 M TBAH-CH_2Cl_2 are summarized in Table IV. As mentioned earlier, compounds **3a-c** can be viewed as derivatives of $W_2Cl_6(dppm)_2$ (**2**), where a terminal chloride ligand has been substituted by an isocyanide. In related systems where substitution of halide by isocyanide has occurred, a shift of the electrochemical processes to more positive potentials is observed for the isocyanide complexes with respect to the original halide precursors.[6] For example, we see this type of shift in the case of $Mo_2X_4(dppm)_2$ (X = Cl, Br, I) upon conversion to the complexes $[Mo_2X_3(dppm)_2(CNR)]PF_6$ (R = *t*-Bu, *i*-Pr).[6] Thus, if we consider complexes **3a-c** as derivatives of $W_2Cl_6(dppm)_2$, then the two processes observed in the CV of the latter complex at $E_{1/2}(ox)$ = +0.79 V and $E_{1/2}(red)$ = -0.91 V vs. Ag/AgCl should shift to more positive potentials in the CV's of **3a-c**. In fact, the oxidation at +0.79 V for **2** shifts to +1.19 V (i.e. by 0.40 V to more positive potentials) while the reduction at -0.91 V in **2** shifts to -0.10 to -0.15 V (i.e. by 0.7-0.8 V to more positive potentials). In addition, another reduction, which appears to be reversible, is observed with $E_{1/2}$ at ca. -1.2 V vs. Ag/AgCl for **3a-c** (Figure 1c); this may be the counterpart of the irreversible process at $E_{p,c} \simeq -1.7$ V vs. Ag/AgCl in the CV of **2**. According to the extended Hückel calculations discussed previously in the case of **2**, both the oxidation and the first reduction processes in complexes **2** and **3** correspond (at least formally) to a change in the bond order from 1 ($\sigma^2\pi^2\delta^{*2}$) to 1.5. However, these are of two distinctly different types, viz. the electron-poor ($\sigma^2\pi^2\delta^{*1}$) and the electron-rich ($\sigma^2\pi^2\delta^{*2}\delta^1$) configurations for the oxidation and reduction, respectively.

As was mentioned earlier in this section, a species of stoichiometry $W_2Cl_5(dppm)_2(CNR)$ may be the precursor to **3** although we were unable to isolate it in pure form from the reaction of **1** with RNC. Also, this same dark brown material (albeit analytically impure) was also obtained in the case of R = xylyl by the chemical reduction (using $(\eta^5\text{-}C_5H_5)_2Co$ in acetone or superhydride in THF) and electrochemical reduction (electrolysis at -0.2 V in 0.2 M TBAH-CH_2Cl_2) of the xylyl isocyanide complex **3b**. There was excellent agreement between the ESR spectra and CV's measured on samples of $W_2Cl_5(dppm)_2(CNxy)$ that were generated both by chemical means and by electrochemical reduction of the cation. The CV of $W_2Cl_5(dppm)_2$-(CNxyl) was identical with that found for the cation of **3b** except that the process at -0.11 V now corresponds to an oxidation. The X-band ESR spectra of frozen solutions of the neutral species in CH_2Cl_2 (-160 °C) exhibit three g values: g_1 = 1.95, g_2 = 1.89, and g_3 = 1.79; g_1 exhibits a phosphorus hyperfine structure ($A \simeq 25$G), but there is no resolvable fine structure associated with either g_2 or g_3 at -160 °C.

The IR spectrum (Nujol mull) of the impure neutral complex has an intense, broad band for $\nu(C{\equiv}N)$ at 2060 cm^{-1}. This represents a shift of 110 cm^{-1} to lower energy from the value of 2170 cm^{-1} found for $\nu(C{\equiv}N)$ in the oxidized complex **3b**. This shift is consistent with the observation in many other systems that π-back-bonding decreases with an increase in metal oxidation state. The decrease of π-back-bonding upon oxidation results in a shift of the $\nu(C{\equiv}N)$ band to higher energy.

In conclusion, we note that the isocyanide-containing species $[W_2Cl_5(dppm)_2(CNR)]^+$ are members of a growing class of multiply bonded dimetal complex that contain π-acceptor CO and RNC ligands and that can be stabilized by intramolecular phosphine bridging ligands.[1-6] Complexes **3a-c** constitute the first such examples for tungsten.

Acknowledgment. We thank the National Science Foundation (Grant No. CHE85-06702) for support of this work. We thank Professor R. E. McCarley for fruitful discussions, for providing us with details of relevant studies underway in his laboratory,[17] and for suggesting alternative strategies for the synthesis of $W_2(\mu\text{-}H)(\mu\text{-}Cl)Cl_4(dppm)_2$. We also thank Professor F. A. Cotton for information concerning the synthesis of $W_2Cl_4(dppm)_2$,[16] Professor T. J. Smith for magnetic susceptibility measurements, and Ju-sheng Qi for experimental assistance.

Supplementary Material Available: Listings of anisotropic thermal parameters (Table S1), bond distances (Table S2), and bond angles (Table S3) and a figure showing the full atomic numbering scheme (Figure S1) (7 pages); a table of observed and calculated structure factors (19 pages). Ordering information is given on any current masthead page.

Contribution from the Department of Chemistry, Purdue University, West Lafayette, Indiana 47907

Binuclear Isocyanide Complexes of Iridium(I). Synthesis, Structure, and Hydrogen Reactivity of $[Ir_2(\mu\text{-}CNR)(CNR)_4(PMe_2CH_2PMe_2)_2][PF_6]_2$ (R = 2,6-$Me_2C_6H_3$, *t*-C_4H_9)

Jianxin Wu, Mark K. Reinking, Phillip E. Fanwick,† and Clifford P. Kubiak*

Received June 17, 1986

The binuclear iridium complexes $[Ir_2(\mu\text{-}CNR)(CNR)_4(PMe_2CH_2PMe_2)_2][PF_6]_2$ (R = 2,6-$Me_2C_6H_3$ (**1**), *t*-C_4H_9 (**3**)) have been synthesized in high yields. Complex **1** crystallizes in the monoclinic space group $P2_1/n$, with a = 19.388 (5) Å, b = 15.193 (5) Å, c = 24.060 (4) Å, β = 94.15 (2)°, and Z = 4. The Ir-Ir separation of 2.7850 (7) Å is consistent with a metal-metal single bond. Complex **1** is fluxional in solution. Variable low-temperature ^1H NMR studies of **1** reveal a dynamic process involving the exchange of isocyanide ligands between bridging and terminal positions. The binuclear iridium(I) complexes, **1** and **3**, react quantitatively with H_2, leading to displacement of one isocyanide ligand and formation of the dihydrides $[Ir_2(\mu\text{-}H)_2(CNR)_4$-$(PMe_2CH_2PMe_2)_2][PF_6]_2$ (R = 2,6-$Me_2C_6H_3$ (**2**), *t*-C_4H_9 (**4**)). Selective ^1H-decoupled ^{31}P NMR experiments have been employed to demonstrate the dihydridic nature of **2** and **4**. The kinetics of the hydrogenation of **1** to **2** has been studied over the temperature range $0 \le T \le 36$ °C. The hydrogenation of complex **1** is first order in [**1**] and zero order in $[H_2]$: $\Delta H^* = 28$ kcal mol^{-1}; $\Delta S^* = 18$ cal mol^{-1} K^{-1}.

We report the preparation of new binuclear isocyanide complexes of iridium bridged by bis(dimethylphosphino)methane (dmpm). The chemistry of mononuclear complexes of Ir has attracted considerable attention becasue of their roles in the activation of C-H bonds,[9-11] CO_2,[12] and H_2.[13] Binuclear com-

†Address correspondence pertaining to crystallographic studies to this author.

(1) Sutherland, B. R.; Cowie, M. *Organometallics* **1985**, *4*, 1637.

0020-1669/87/1326-0247$01.50/0

plexes of Ir, particularly those bridged by the diphosphine bis(diphenylphosphino)methane (dppm), have also been investigated by several groups.[1-3] The aim of these latter studies generally has been to explore bimetallic participation in the activation of small molecules. The phenyl rings of the dppm ligand however appear to limit metal-centered reactivity in dppm complexes.[14] Recently, therefore, we[5] and others[6-8] have sought to exploit the lesser steric requirements and greater donor ability of the dmpm ligand in preparing binuclear complexes. We report herein the first dmpm-bridged diiridium complexes, $[Ir_2(\mu\text{-CNR})(CNR)_4(dmpm)_2][PF_6]_2$ (R = 2,6-Me_2-C_6H_3, *t*-C_4H_9), the solution and solid-state structure of the 2,6-xylyl isocyanide derivative, and the reactivity of these new complexes with H_2.

Experimental Section

Materials and Physical Measurements. All preparations were done under an atmosphere of dry N_2. Solvents were reagent grade and were distilled from the appropriate drying agents. The ligand *t*-BuNC was prepared by a literature method.[15] The ligand dmpm was prepared as described previously.[5b] $[Ir(COD)Cl]_2$[24] and $[Ir(COD)_2][PF_6]$[25] were prepared by literature procedures. ^1H NMR spectra were recorded on Nicolet 470 and Varian XL-200 spectrometers. ^{31}P NMR spectra were recorded on a Varian XL-200 spectrometer operating at 81 MHz with broad-band proton decoupling. The ^{31}P chemical shifts are reported relative to 85% H_3PO_4. Infrared spectra were recorded on a Perkin-Elmer 1710 FTIR. Melting points were measured on a Fisher melting point apparatus. UV-vis spectra were measured on Hewlett-Packard 8450A and 8451 diode array spectrophotometers.

Preparation of $[Ir_2(CN\text{-}2,6\text{-}Me_2C_6H_3)_5(dmpm)_2][PF_6]_2\cdot 2CH_2Cl_2$ (1). $[Ir(COD)Cl]_2$ (0.778 g, 1.16 mmol) was dissolved in 25 mL of CH_2Cl_2. To this was slowly added a solution of 2,6-xylyl isocyanide (1.22 g, 9.30 mmol) in 25 mL of CH_2Cl_2 to give a dark green solution. After the solution was stirred under N_2 for 1 h, CH_2Cl_2 was evaporated under vacuum. To the remaining dark green residue was added 20 mL of ethanol to dissolve the solids. Bis(dimethylphosphino)methane (0.35 g, 2.57 mmol) was added dropwise to give a yellow solution. After this solution was stirred for 3 h, a solution of predried NH_4PF_6 (0.75 g, 4.60 mmol) in 10 mL of ethanol was added to afford a yellow precipitate. The solid was collected by filtration, washed with ethanol three times, and dried under vacuum. The solid was recrystallized from CH_2Cl_2/Et_2O to give 1.60 g (86%) of crystalline product, solvated by two molecules of methylene chloride. The existence of CH_2Cl_2 was confirmed by ^1H NMR in CD_3CN as well as by an X-ray structure determination. Anal. Calcd for $C_{57}H_{77}N_5P_6Cl_4F_{12}Ir_2$: C, 38.63; H, 4.38; N, 3.95. Found: C, 38.63; H, 4.68; N, 4.30. ^1H NMR (CD_2Cl_2): δ 7.18 (m, 15 H), 3.10 (p, 4 H), 2.43 (s, 30 H), 2.03 (s, 24 H). $^{31}P\{^1H\}$ NMR (CD_2Cl_2): δ −44.06 (s), −143.1 (septet, PF_6^-). IR (KBr): ν(CN) 2167 (sh), 2121 (s), 2101 (s), 1639 (s), 1585 (m) cm^{-1}. UV-vis (CH_3CN): 313 nm (ϵ 25 400), 400 nm (ϵ 2640). Mp: 233–235 °C.

Preparation of $[Ir_2(\mu\text{-}H)_2(CN\text{-}2,6\text{-}Me_2C_6H_3)_4(dmpm)_2][PF_6]_2$ (2). Complex **1** (0.20 g, 0.11 mmol) was dissolved in 25 mL of THF. The solution was heated to reflux under an atmosphere of H_2. After 5 h, the volume of the solution was decreased to ca. 10 mL, with formation of a pale yellow precipitate. The moderately air-stable solid was collected by vacuum filtration, washed with 0.3 mL THF and then with Et_2O, and dried under vacuum. Isolated yield: 0.15 g (~80%). Complex **2** has one CH_2Cl_2 of solvation, as confirmed by ^1H NMR in CD_3CN. Anal. Calcd for $C_{47}H_{66}N_4P_6Cl_2F_{12}Ir_2$: C, 36.23; H, 4.27; N, 3.60. Found: C, 36.50; H, 4.46; N, 3.71. ^1H NMR (CD_3CN): δ 7.25 (m, 12 H), 5.30 (s, 2 H), 3.90 (t, 4 H, $J_{P\text{-}H}$ = 4.5 Hz), 2.54 (s, 24 H), 2.02 (s, 24 H), −11.96 (p, 2 H, $J_{P\text{-}H}$ = 8.3 Hz). $^{31}P\{^1H\}$ NMR (CD_2Cl_2): δ −49.1 (s), −143.1 (septet, PF_6^-). IR (KBr): ν(CN) 2146 (s), 2127 (s), 1995 (w) cm^{-1}.

Preparation of $[Ir_2(CN\text{-}t\text{-}Bu)_5(dmpm)_2][PF_6]_2$ (3). $[Ir(COD)_2][PF_6]$ (0.202 g, 0.36 mmol) was dissolved in 10 mL of CH_2Cl_2. To this solution was added an excess of *tert*-butyl isocyanide (0.20 mL, 1.77 mmol), causing the solution to change color from purple to yellow. The ligand dmpm (0.056 mL, 0.36 mmol) then was added, and the solution was stirred for 1 h. Diethyl ether was added to initiate precipitation of a yellow powder, which was collected on a frit, washed with diethyl ether, and dried under vacuum. Isolated yield: 0.22 g (88%). Anal. Calcd for $C_{35}H_{73}N_5P_6F_{12}Ir_2$: C, 30.85; H, 5.41; N, 5.14. Found: C, 30.12; H, 5.68; N, 5.16. ^1H NMR (CD_3CN): δ 2.52 (p, 4 H), 1.83 (s, 24 H), 1.49 (s, 45 H). $^{31}P\{^1H\}$ NMR (CD_3CN): δ −45.84 (s), −143.1 (septet, PF_6^-). IR (CH_2Cl_2): ν(CN) 2148 (s), 2125 (s), 2051 (w), 1640 (s), 1587 (w) cm^{-1}.

Preparation of $[Ir_2(\mu\text{-}H)_2(CN\text{-}t\text{-}Bu)_4(dmpm)_2][PF_6]_2$ (4). Complex **3** (0.17 g, 0.12 mmol) was dissolved in 10 mL of CH_3CN. The solution was stirred under an atmosphere of H_2 at room temperature for 48 h, causing the yellow solution to turn pale yellow. Diethyl ether was added to initiate precipitation of the white solid, which was collected on a frit, washed with diethyl ether, and dried under vacuum. Isolated yield: 0.11 g (70%). Anal. Calcd for $C_{30}H_{66}N_4P_6F_{12}Ir_2$: C, 28.12; H, 5.20; N, 4.37. Found: C, 27.29; H, 5.64; N, 4.09. ^1H NMR (CD_3CN): δ 3.61 (p, 4 H), 1.89 (s, 24 H), 1.54 (s, 36 H), −12.95 (p, 2 H, $J_{P\text{-}H}$ = 8.0 Hz). $^{31}P\{^1H\}$ NMR (CD_3CN): δ −50.6 (s), −143.1 (septet, PF_6^-). IR (CH_3CN): ν(CN) 2168 (s), 2147 (s), 2051 (w) cm^{-1}.

Kinetics of Hydrogenation of 1. The kinetics for the hydrogenation of **1** to give **2** was studied at 0, 13, 25, and 36 °C. Kinetic data were obtained by monitoring the disappearance of absorbance of **1** at 2100 cm^{-1} by FTIR (Figure 4). At 25 °C, three solutions with the same initial concentration of **1**, 4×10^{-4} M, were charged with H_2 to 1, 0.5, and 0.25 atm, respectively. Total pressures were adjusted to 1 atm by addition of N_2. Partial pressures of H_2 were verified by gas chromatographic analysis on a Carle S-0158 instrument. The concentration of H_2 in the THF was calculated from literature solubility data.[23] IR spectra of each solution were taken at fixed time intervals during the reaction, and the absorbances at 2100 cm^{-1} were compared. All were identical within experimental error. Thus, the reaction rate is not dependent on $[H_2]$. At 25 °C, with $[\mathbf{1}]_0 = 2.7 \times 10^{-3}$ M and $[H_2]_0 = 4.0 \times 10^{-3}$ M,[23] the disappearance of absorbance of **1** at 2100 cm^{-1} was monitored by FTIR. A first-order plot of ln $(A_t - A_\infty)$ at 2100 cm^{-1} for **1** vs. time gave an excellent straight line over 3 half-lives. Over the temperature range 0–36 °C, reaction rate constants were obtained from first-order plots of ln $(A_t - A_\infty)$ at 2100 cm^{-1} for **1** vs. time. The rate constants measured are given in Table IV. A plot of ln (k/T) vs. T^{-1} gave a straight line with slope = −14 000, intercept = 32.75, and correlation = 0.9950. Activation parameters for the hydrogenation of **1** are $\Delta H^* = 28$ kcal mol^{-1} and $\Delta S^* = 18$ cal mol^{-1} K^{-1}.

Crystal Data Collection and Reduction. A yellow needle-shaped crystal measuring 0.59 × 0.33 × 0.06 mm was used for determination of cell parameters and subsequent data collection. The crystal was mounted on a glass fiber with epoxy and transferred to the diffractometer. Crystal survey, determination of cell constants, and subsequent data collection

(2) Kubiak, C. P.; Woodcock, C.; Eisenberg, R. *Inorg. Chem.* **1980**, *29*, 2733.
(3) Mague, J. T.; Sanger, A. R. *Inorg. Chem.* **1979**, *18*, 2060.
(4) Hunt, C. T.; Balch, A. L. *Inorg. Chem.* **1981**, *20*, 2267.
(5) (a) Kullberg, M. L.; Lemke, F. R.; Powell, D. R.; Kubiak, C. P. *Inorg. Chem.* **1985**, *24*, 3589. (b) Kubiak, C. P.; Kullberg, M. L.; Lemke, F. R.; Raghuveer, K. S.; King, C.; Roundhill, D. M., submitted for publication in *Inorg. Synth.* (c) Kullberg, M. L.; Kubiak, C. P. *Inorg. Chem.* **1986**, *25*, 26. (d) Lemke, F. R.; Kubiak, C. P. *J. Chem. Soc., Chem. Commun.* **1985**, 1729. (e) Lemke, F. R.; Kubiak, C. P. *Inorg. Chim. Acta* **1986**, *113*, 125.
(6) (a) Ling, S. S. M.; Puddephatt, R. J.; Manojlovic-Muir, L.; Muir, K. W. *J. Organomet. Chem.* **1983**, 255, C11. (b) Ling, S. S.; Puddephatt, R. J.; Manojlovic-Muir, L.; Muir, K. W. *Inorg. Chim. Acta* **1983**, *77*, L95. (c) Manojlovic-Muir, L.; Muir, K. W.; Frew, A. A.; Ling, S. S. M.; Thomson, M. A.; Puddephatt, R. J. *Organometallics* **1984**, *3*, 1637.
(7) Karsch, H. H.; *Z. Naturforsch., B: Anorg. Chem., Org. Chem.* **1983**, *38B*, 1027.
(8) King, R. B.; RaghuVeer, K. S. *Inorg. Chem.* **1984**, *23*, 2482.
(9) Fryzuk, M. D.; MacNeil, P. A.; Rettig, S. J. *J. Am. Chem. Soc.* **1985**, *107*, 6708.
(10) Janowicz, A. H.; Bergman, R. G. *J. Am. Chem. Soc.* **1983**, *105*, 3929.
(11) Fisher, B.; Eisenberg, R. *Organometallics* **1983**, *2*, 764.
(12) (a) Harlow, R. L.; Kinney, J. B.; Herskovitz, T. *J. Chem. Soc., Chem. Commun.* **1980**, 813. (b) Calabrese, J. C.; Herskovitz, T.; Kinney, J. B. *J. Am. Chem. Soc.* **1983**, *105*, 5914.
(13) Johnson, C. E.; Eisenberg, R. *J. Am. Chem. Soc.* **1985**, *107*, 3148.
(14) Sutherland, B. R.; Cowie, M., submitted for publication in *Can. J. Chem.*
(15) Weber, W. P.; Gokel, G. W.; Ugi, I. K. *Angew. Chem., Int. Ed. Engl.* **1972**, *11*, 530.
(16) Shanan-Atidi, H.; Bar-Eli, K. H. *J. Phys. Chem.* **1970**, *74*, 961.
(17) Puddephatt, R. J. *Chem. Soc. Rev.* **1983**, *12*, 99.
(18) Kullberg, M. L.; Lemke, F. R.; Powell, D. R.; Kubiak, C. P. *Inorg. Chem.* **1985**, *24*, 3589.
(19) DeLaet, D. L.; Powell, D. R.; Kubiak, C. P. *Organometallics* **1985**, *4*, 954.
(20) (a) Pierpont, C. G.; Stuntz, G. F.; Shapley, J. R. *J. Am. Chem. Soc.* **1978**, 616. (b) Shapley, J. R.; Stuntz, G. F.; Churchill, M. R.; Hutchinson, J. P. *J. Am. Chem. Soc.* **1979**, *101* 7425.
(21) Hoffman, D. M.; Hoffmann, R. *Inorg. Chem.* **1981**, *20*, 3543.
(22) Rankin, D. W. H.; Robertson, H. E.; Karsch, H. H. *J. Mol. Struct.* **1981**, *77*, 121.
(23) Young, C. L., Ed. *Solubility Data Ser.* **1981**, *5–6*, 219.
(24) Herde, J. L.; Lambert, J. C.; Senott, C. V. *Inorg. Synth.* **1974**, *15*, 18.
(25) Green, M.; Kuc, T. A.; Taylor, S. H. *J. Chem. Soc. A* **1971**, 2336.

Table I. Summary of Crystal Data and Collection Parameters for $[Ir_2(\mu\text{-CNR})(CNR)_4(dmpm)_2][PF_6]_2(CH_2Cl_2)_2$ (R = 2,6-Me_2-C_6H_3)

formula	$Ir_2Cl_4P_6F_{12}N_5C_{57}H_{77}$
fw	1772.32
space gp	$P2_1/n$
a, Å	19.388 (5)
b, Å	15.193 (5)
c, Å	24.060 (4)
β, deg	94.15 (2)
V, Å^3	7069 (6)
Z	4
d_{calcd}, g cm^{-3}	1.665
cryst dimens, mm	0.59 × 0.33 × 0.06
temp, °C	27.0
radiation (wavelength)	Mo Kα (0.71073 Å)
monochromator	graphite
linear abs coeff, cm^{-1}	41.03
abs corr applied	empirical[a]
cryst radius, cm	0.028
diffractometer	Enraf-Nonius CAD4
scan method	θ–2θ
h, k, l limits	0 to +15, 0 to +16, −25 to +25
2θ range, deg	3.00–45.00
scan width, deg	0.70 + 0.35 tan θ
takeoff angle, deg	5.00
programs used	Enraf-Nonius SDP
F_{000}	3496.0
unique data	8459
data with $I > 3.0\sigma(I)$	5710
no. of variables	571
largest shift/esd in final cycle	0.67
R	0.057
R_w	0.072
goodness of fit	1.704

[a] Flack, H. D. *Acta Crystallogr., Sect. A* **1977**, *A33*, 890.

were performed on a Enraf-Nonius CAD-4 automated single-crystal diffractometer using a graphite monochromator and Mo Kα (λ = 0.71073 Å) radiation at 27 °C. The unit cell was assigned to space group $P2_1/n$. Cell parameters were determined from a least-squares refinement of 24 intense, high-angle reflections.

Data were collected over the following hkl limits: $0 \le h \le 15$, $0 \le k \le 16$, $-25 \le l \le 25$; in the range $3 \le 2\theta \le 45°$. Three standard reflections were monitored every 100 observations, and the intensities showed no significant trends over data collection. The linear absorption coefficient for Mo Kα radiation is 41.03 cm^{-1}, and an empirical absorption correction, based on a series of ψ-scans, was applied to the data. The final data set consisted of 8459 unique reflections of which 5710 had $I > 3\sigma(I)$.

Solution and Refinement of the Structure. The structure was solved by the MULTAN 11/82 program package and refined by full-matrix least-squares methods in the space group $P2_1/n$. The space group $P2_1/n$ is a nonstandard setting of $P2_1/c$ (No. 14). Convergence of the full-matrix least-squares refinement gave residuals R = 0.057 and R_w = 0.072. In all refinements the function minimized was $\sum w(|F_o| - |F_c|)^2$, where $w = 1/\sigma^2(F)$. Corrections for anomalous dispersion were applied to all anisotropically refined atoms. No correction was made for primary or secondary extinction. The value of p used in the weighting was 0.07. All programs used were from the SDP program library, and all calculations were carried out on a PDP 11/34 computer in the Chemical X-ray Diffraction Facility at Purdue University.

A summary of crystal data and collection parameters appears in Table I. Positional and thermal parameters are listed in Table II. Bond distances and angles are given in Table III.

Results and Discussion

The new dmpm-bridged isocyanide complexes of iridium $[Ir(CNR)_5(dmpm)_2][PF_6]_2$ (R = 2,6-$Me_2C_6H_3$ (**1**), *t*-Bu (**3**)) have been prepared. Complexes **1** and **3** were prepared by in situ formation of $Ir(CNR)_4^+$ followed by reaction with dmpm and metathesis with PF_6^-. Isolated yields are generally 80–90%. The xylyl isocyanide derivative, **1**, exhibits terminal ν(CN) at 2167 (sh), 2121 (s), and 2101 (s) cm^{-1} as well as a bridging ν(CN) = 1639 cm^{-1} and an additional weaker band at 1585 cm^{-1}. The $^{31}P\{^1H\}$ NMR signal appears as a singlet at temperatures as low as −50 °C, consistent with a symmetric structure. The corresponding *t*-Bu derivative, **3**, is characerized by systematically lower

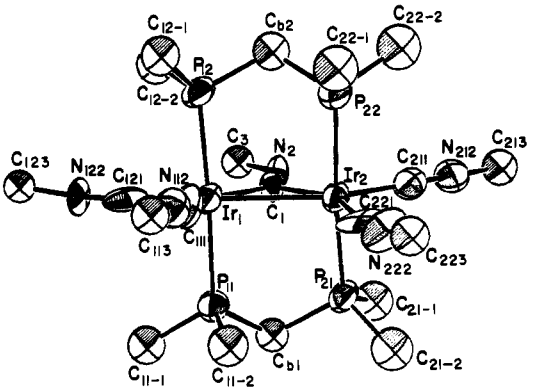

Figure 1. ORTEP drawing of the $[Ir_2(\mu\text{-CNR})(CNR)_4(dmpm)_2]^{2+}$ (R = 2,6-Me_2-C_6H_3) molecular cation of **1** showing 50% probability thermal ellipsoids. For clarity, only the ipso 2,6-xylyl carbon atoms bonded to isocyanide N atoms have been included.

terminal ν(CN) = 2148 (s), 2125 (s), and 2051 (w) cm^{-1} as well as a bridging isocyanide evident at 1640 cm^{-1} and a weak band at 1587 cm^{-1}. The $^{31}P\{^1H\}$ NMR signal of **3** is also a singlet. The spectroscopic and analytical data for **1** and **3** indicate that they are symmetric $(dmpm)_2Ir^I_2$ complexes with one bridging and four terminal isocyanide ligands, structure I. An apparently analogous

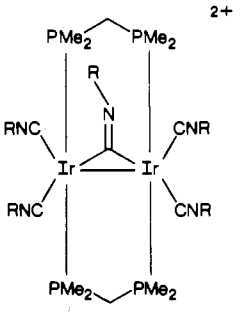

I (R=2,6-Me_2-C_6H_3 (1), *t*-Bu (3))

carbonyl complex was recently reported by Sutherland and Cowie.[1] The structure of **1** was confirmed by an X-ray diffraction study, which is described below.

Solid-State Structure of $[Ir_2(\mu\text{-CN-2,6-}Me_2C_6H_3)(CN\text{-2,6-}Me_2C_6H_3)_4(dmpm)_2][PF_6]_2\cdot 2CH_2Cl_2$. The crystal structure of **1** is composed of $[Ir_2(\mu\text{-CNR})(CNR)_4(dmpm)]^{2+}$ cations and well-separated PF_6^- anions. There are two CH_2Cl_2 molecules of crystallization per asymmetric unit. The structure of the molecular ion **1** consists of the now familiar *trans,trans*-bis(diphosphine) binuclear framework, typical of the A-frames and related molecules.[1,2,17,18] The two Ir atoms are bridged by a pair of mutually trans dmpm ligands and a 2,6-xylyl isocyanide ligand. The two iridium atoms and one bridging and four terminal isocyanides lie approximately in a plane perpendicular to the four dmpm phosphorus atoms. The $[Ir_2(\mu\text{-CNR})(CNR)_4(dmpm)_2]^{2+}$ (R = 2,6-$Me_2C_6H_3$) ion possesses no crystallographically imposed elements of symmetry. The complex **1** can be viewed as a bis exo adduct of an isocyanide-bridged Ir(I) A-frame. It is interesting to note the relationship of this structure to $[Ni_2(\mu\text{-CNMe})(CNMe)_3(dppm)]^{2+}$, a mono exo adduct of an isocyanide-bridged Ni(I) A-frame with the same valence-electron count.[19] An ORTEP drawing of the molecular cation $[Ir_2(\mu\text{-CNR})(CNR)_4(dmpm)_2]^{2+}$ (R = 2,6-$Me_2C_6H_3$) with the xylyl groups omitted is given in Figure 1.

The coordination geometry about each Ir atom is approximately square pyramidal, with the single bridging isocyanide serving as the common vertex to the overall corner-shared bi-square-pyramidal type structure. The trans angles about Ir1 are P12–Ir1–P11, 177.2 (1)°, and C1–Ir1–C11, 150.6 (5)°, and at Ir2 are P22–Ir2–P21, 173.4 (1)°, and C1–Ir2–C221, 151.6 (6)°. The exo isocyanide carbon atom, C121, forms the apex of the square pyramid at Ir1 and exhibits cis angles through Ir1 of 99.1 (5), 91.7 (4), 94.1 (5), and 110.4 (5)° to C111, P11, P12, and C1,

Table II. Positional and Thermal Parameters and Their Estimated Standard Deviations for $[Ir_2(\mu\text{-CNR})(CNR)_4(dmpm)_2][PF_6]_2(CH_2Cl_2)_2$ (R = 2,6-Me_2-C_6H_3)[a]

atom	x	y	z	B, Å²	atom	x	y	z	B, Å²
Ir1	0.30865 (3)	0.27324 (4)	−0.03911 (3)	3.30 (1)	C128	0.6574 (8)	0.475 (1)	0.1772 (7)	4.6 (4)*
Ir2	0.30389 (3)	0.15041 (4)	0.04645 (3)	0.35 (1)	C129	0.494 (1)	0.619 (2)	0.167 (1)	9.0 (6)
P11	0.2831 (2)	0.1587 (3)	−0.1024 (2)	3.92 (9)	C1210	0.7286 (9)	0.474 (2)	0.157 (1)	7.7 (6)
P12	0.3350 (2)	0.3916 (3)	0.0202 (2)	4.4 (1)	C211	0.3485 (8)	0.078 (1)	0.1052 (7)	4.2 (4)
P21	0.3170 (2)	0.0289 (3)	−0.0108 (2)	4.1 (1)	N212	0.3783 (7)	0.0353 (9)	0.1389 (5)	4.9 (3)
P22	0.3006 (3)	0.2649 (3)	0.1108 (2)	5.1 (1)	C213	0.4169 (9)	−0.016 (1)	0.1796 (7)	5.2 (4)*
C-B1	0.3263 (8)	0.055 (1)	−0.0840 (7)	4.2 (3)*	C214	0.487 (1)	0.007 (1)	0.1911 (9)	6.8 (5)*
C-B2	0.3524 (9)	0.360 (1)	0.0939 (7)	5.2 (4)*	C215	0.525 (1)	−0.054 (2)	0.231 (1)	8.2 (6)*
C11-1	0.8045 (9)	0.323 (1)	0.3261 (8)	5.4 (4)*	C216	0.489 (1)	−0.120 (2)	0.252 (1)	9.7 (7)*
C11-2	0.1908 (9)	0.129 (1)	−0.1113 (8)	5.8 (4)*	C217	0.423 (1)	−0.141 (2)	0.239 (1)	9.4 (7)*
C12-1	0.2693 (9)	0.477 (1)	0.0180 (7)	5.3 (4)*	C218	0.382 (1)	−0.089 (1)	0.1997 (8)	6.6 (5)*
C12-2	0.4141 (9)	0.450 (1)	0.0069 (8)	5.8 (4)*	C219	0.980 (1)	0.580 (2)	0.334 (1)	8.9 (7)
C21-1	0.397 (1)	−0.033 (1)	0.0052 (8)	6.1 (4)*	C2110	0.193 (1)	0.393 (2)	0.317 (1)	8.8 (7)
C21-2	0.249 (1)	−0.054 (1)	−0.0096 (8)	6.6 (5)*	C221	0.204 (1)	0.128 (1)	0.0493 (8)	6.2 (4)
C22-1	0.214 (1)	0.309 (1)	0.1230 (9)	6.8 (5)*	N222	0.1422 (6)	0.116 (1)	0.0585 (7)	5.7 (4)
C22-2	0.337 (1)	0.241 (1)	0.1813 (9)	7.3 (5)*	C223	0.0741 (8)	0.109 (1)	0.0707 (7)	4.9 (4)*
C1	0.3869 (8)	0.2039 (9)	0.0088 (6)	3.6 (3)	C224	0.0247 (9)	0.119 (1)	0.0291 (7)	5.3 (4)*
N2	0.4512 (6)	0.1976 (8)	0.0208 (5)	3.4 (3)	C225	−0.047 (1)	0.110 (1)	0.0422 (9)	6.7 (5)*
C3	0.5110 (8)	0.238 (1)	−0.0012 (7)	4.5 (3)*	C226	−0.058 (1)	0.099 (2)	0.0970 (9)	7.7 (5)*
C4	0.5568 (9)	0.278 (1)	0.0380 (7)	5.2 (4)*	C227	−0.011 (1)	0.092 (2)	0.137 (1)	8.1 (6)*
C5	0.6213 (9)	0.308 (1)	0.0211 (7)	5.3 (4)*	C228	0.062 (1)	0.098 (1)	0.1256 (9)	6.9 (5)*
C6	0.639 (1)	0.296 (1)	−0.0298 (9)	7.0 (5)*	C229	0.040 (1)	0.132 (1)	−0.0319 (9)	6.9 (6)
C7	0.5922 (9)	0.253 (1)	−0.0721 (7)	5.2 (4)*	C2210	0.382 (1)	0.592 (2)	0.327 (1)	10.5 (8)
C8	0.5277 (8)	0.222 (1)	−0.0560 (7)	4.5 (3)*	P1	0.7477 (3)	0.6479 (4)	0.3066 (2)	6.6 (1)
C9	0.541 (1)	0.293 (1)	0.0977 (9)	6.6 (5)	F11	0.724 (1)	0.641 (1)	0.2454 (7)	15.4 (6)
C10	0.4823 (8)	0.169 (1)	−0.0968 (8)	5.3 (5)	F12	0.718 (1)	0.739 (1)	0.3128 (8)	19.0 (6)
C111	0.2119 (8)	0.307 (1)	−0.0538 (7)	4.9 (3)	F13	0.788 (1)	0.561 (1)	0.3008 (7)	15.3 (5)
N112	0.1539 (7)	0.3328 (9)	−0.0618 (6)	4.9 (3)	F14	0.808 (1)	0.694 (1)	0.285 (1)	18.5 (8)
C113	0.0840 (8)	0.361 (1)	−0.0759 (7)	4.6 (4)*	F15	0.6997 (9)	0.600 (2)	0.334 (1)	28.2 (8)
C114	0.067 (1)	0.372 (1)	−0.1307 (8)	6.5 (5)*	F16	0.777 (2)	0.651 (1)	0.3639 (8)	24 (1)
C115	−0.005 (1)	0.403 (2)	−0.1454 (9)	7.6 (5)*	P2	0.2574 (4)	0.5847 (4)	0.1851 (3)	7.7 (2)
C116	−0.045 (1)	0.416 (2)	−0.1021 (9)	7.4 (5)*	F21	0.305 (1)	0.656 (1)	0.2121 (8)	16.2 (6)
C117	−0.026 (1)	0.407 (2)	−0.0474 (9)	7.7 (5)*	F22	0.239 (1)	0.646 (2)	0.139 (1)	20.7 (9)
C118	0.044 (1)	0.378 (1)	−0.0322 (8)	6.0 (4)*	F23	0.192 (1)	0.614 (2)	0.2068 (8)	22.1 (8)
C119	0.113 (1)	0.356 (2)	−0.1781 (8)	6.9 (6)	F24	0.268 (1)	0.535 (2)	0.2338 (9)	28.6 (7)
C1110	0.068 (1)	0.364 (2)	0.027 (1)	8.5 (7)	F25	0.3195 (8)	0.553 (1)	0.161 (1)	23.9 (9)
C121	0.6495 (8)	0.654 (1)	0.0980 (7)	4.8 (4)	F26	0.2145 (9)	0.515 (1)	0.1542 (9)	15.7 (6)
N122	0.6276 (7)	0.6085 (9)	0.1292 (5)	4.7 (3)	Cl11	0.8928 (4)	0.4124 (5)	0.1036 (3)	11.9 (2)
C123	0.6104 (8)	0.540 (1)	0.1642 (6)	4.0 (3)*	Cl12	0.8231 (4)	0.3027 (6)	0.0210 (1)	13.4 (3)
C124	0.5433 (9)	0.542 (1)	0.1825 (8)	5.7 (4)*	C-S1	0.858 (2)	0.307 (2)	0.087 (1)	12 (1)
C125	0.524 (1)	0.471 (1)	0.2180 (9)	6.9 (5)*	Cl21	0.3523 (5)	0.3619 (8)	0.3996 (4)	16.2 (4)
C126	0.573 (1)	0.407 (1)	0.2309 (9)	7.1 (5)*	Cl22	0.4443 (5)	0.3307 (7)	0.3175 (4)	15.5 (3)
C127	0.6374 (9)	0.407 (1)	0.2139 (8)	5.9 (4)*	C-S2	0.379 (2)	0.298 (2)	0.349 (1)	16 (1)

[a] Starred values indicate that the atoms were refined isotropically. Anisotropically refined atoms are given in the form of the isotropic equivalent thermal parameter defined as $(4/3)[a^2B(1,1) + b^2B(2,2) + c^2B(3,3) + ab(\cos\gamma)B(1,2) + ac(\text{cis}\ \beta)B(1,3) + bc(\cos\alpha)B(2,3)]$.

respectively. The corresponding cis angles from C211 through Ir2 are 105.4 (6), 85.4 (4), 88.4 (4), and 102.8 (5)° to C221, P21, P22, and C1, respectively.

The Ir–Ir separation of 2.7850 (7) Å is well within the range normally reported for Ir–Ir single bonds.[2,20] The presence of an Ir–Ir bond is consistent with a net 17-valence-electron count at each metal center. However, the bond does not appear to exert a significant stereochemical influence on the molecular structure. This can be understood to arise from a spatially diffuse Ir–Ir bonding MO.[21] The Ir–Ir separation is somewhat shorter than the average nonbonded diphosphine P···P distance, 3.007 Å. The nonbonded P···P distance is only slightly compressed relative to that of the free dmpm ligand in the gas phase, 3.129 Å.[22] The average P–C–P angle for the bridging dmpm methylene carbons is 110.67 (7)°, slightly more acute than ~115° for dmpm in the gas phase.[22] Thus, there appears to be relatively little strain in the eight-membered $Ir_2P_4C_2$ ring.

The remainder of bond distances and angles in the structure appear normal. The average Ir–P distance of the dmpm ligands is 2.333 (6) Å. This agrees quite well with other determined iridium phosphine structures and is slightly longer than the Ir–P distances found in two related dppm-bridged iridium structures, $Ir_2(CO)_2(\mu\text{-OH·Cl})(dppm)_2$, 2.320 (7) Å,[1] and $Ir_2(CO)_3(\mu\text{-S})(dppm)_2$, 2.321 (2) Å.[2] The Ir–C bond lengths for the four terminal isocyanide ligands range from 1.94 (2) to 2.01 (2) Å and are significantly shorter than the μ-isocyanide Ir–C average bond length, 2.10 (2) Å. The bond angle through the bridging isocyanide, Ir1–C1–Ir2, is 83.4 (3)°. The μ-isocyanide is distinctly bent, C1–N2–C3 = 134 (2)°, relative to the essentially linear terminal isocyanides, which display an average C–N–C = 175 (4)°. There are no unusual intermolecular or ionic contacts. The PF_6^- counterions exhibit relatively high thermal parameters for the F atoms, typical of such symmetric ions, but could not be fit to a static disorder model. The two independent CH_2Cl_2 molecules of crystallization also exhibit high thermal parameters. The crystals of **1** grown in CH_2Cl_2/Et_2O do appear to slowly lose their CH_2Cl_2's of crystallization. This may account for the observed thermal behavior of the CH_2Cl_2 molecules in the structure. However, lacking a quantitative measure of CH_2Cl_2 loss, we refined these molecules at full occupancy.

Solution Structure of $[Ir_2(\mu\text{-CNR})(CNR)_4(dmpm)_2]^{2+}$ (R = 2,6-Me_2-C_6H_3). Variable-temperature 470-MHz ^1H NMR studies of **1** indicate that a dynamic process equilibrates the dmpm methyl groups and the 2,6-xylyl isocyanide ligands. At room temperature, a singlet at δ 2.03 is assigned to the methyl protons of the dmpm ligands, while a singlet at δ 2.43 is assigned to the methyl protons of the five xylyl isocyanides. Gradual cooling of the sample resulted in significant broadening of the dmpm methyl singlet, and as the temperature was lowered to −26 °C, this peak was split into two peaks at δ 1.92 and 2.12 (Figure 2). From the coalescence temperature of −2 °C (±5 °C), k = 206 s^{-1} and $\Delta G^{\ddagger}$ = 12.9 ± 0.3 kcal mol^{-1} were obtained for the equilibration of dmpm methyl environments. At significantly lower temperatures, distinct isocyanide ligand environments could be observed. The

Table III. Selected Bond Distances and Angles for $[Ir_2(\mu\text{-CNR})(CNR)_4(dmpm)_2][PF_6]_2$ (R = 2,6-Me_2-C_6H_3)[a]

	(a) Bond Distances (Å)		
Ir1–Ir2	2.7850 (7)	P21–C-B1	1.83 (1)
Ir1–P11	2.342 (3)	P21–C21-1	1.84 (2)
Ir1–P12	2.329 (4)	P21–C21-2	1.82 (2)
Ir1–C1	2.12 (1)	P22–C-B2	1.82 (1)
Ir1–C111	1.95 (1)	P22–C22-1	1.85 (2)
Ir1–C121	2.01 (2)	P22–C22-2	1.83 (2)
Ir2–P21	2.328 (3)	C1–N2	1.26 (1)
Ir2–P22	2.333 (4)	N2–C3	1.45 (2)
Ir2–C1	2.07 (1)	C111–N112	1.19 (2)
Ir2–C211	1.94 (2)	N112–C113	1.45 (2)
Ir2–C221	1.97 (2)	C121–N122	1.12 (2)
P11–C-B1	1.82 (1)	N122–C123	1.39 (2)
P11–C11-1	1.82 (1)	C221–N222	1.25 (2)
P11–C11-2	1.84 (1)	N222–C223	1.38 (2)
P12–C-B2	1.85 (1)	C211–N212	1.16 (2)
P12–C12-1	1.82 (1)	N212–C213	1.42 (2)
P12–C12-2	1.82 (2)		
	(b) Bond Angles (deg)		
Ir2–Ir1–P11	88.08 (9)	C11-1–P11–C11-2	102.3 (7)
Ir2–Ir1–P12	94.68 (9)	Ir1–P12–C-B2	113.8 (5)
Ir2–Ir1–C111	103.2 (4)	Ir1–P12–C12-1	114.4 (5)
Ir2–Ir1–C121	157.6 (4)	Ir1–P12–C12-2	114.9 (6)
P11–Ir1–P12	177.2 (1)	C-B2–P12–C12-1	107.1 (7)
P11–Ir1–C1	95.4 (3)	C-B2–P12–C12-2	101.5 (7)
P11–Ir1–C111	85.6 (5)	C12-1–P12–C12-2	104.0 (7)
P11–Ir1–C121	91.7 (4)	Ir2–P21–C-B1	114.9 (4)
P12–Ir1–C1	86.3 (3)	Ir2–P21–C21-1	114.3 (6)
P12–Ir1–C111	94.1 (5)	Ir2–P21–C21-2	115.1 (5)
P12–Ir1–C121	85.8 (4)	C-B1–P21–C21-1	100.1 (6)
C1–Ir1–C111	150.6 (5)	C-B1–P21–C21-2	106.7 (7)
C1–Ir1–C121	110.4 (5)	C21-1–P21–C21-2	104.3 (7)
C111–Ir1–C121	99.1 (5)	Ir2–P22–C-B2	113.6 (5)
Ir1–Ir2–P21	94.75 (9)	Ir2–P22–C22-1	116.2 (6)
Ir1–Ir2–P22	89.7 (1)	Ir2–P22–22-2	116.3 (6)
Ir1–Ir2–C211	151.6 (4)	C-B2–P22–C22-1	105.8 (7)
Ir1–Ir2–C221	103.0 (5)	C-B2–P22–C22-2	100.2 (7)
P21–Ir2–P22	173.4 (1)	C22-1–P22–C22-2	102.8 (8)
P21–Ir2–C1	86.0 (3)	P11–C-B1–P21	110.3 (7)
P21–Ir2–C211	85.4 (4)	P12–C-B2–P22	110.9 (7)
P21–Ir2–C221	92.0 (4)	Ir1–C1–Ir2	83.4 (5)
P22–Ir2–C1	93.3 (3)	Ir1–C1–N2	144.9 (9)
P22–Ir2–C211	88.4 (4)	Ir2–C1–N2	131.0 (8)
P22–Ir2–C221	91.8 (4)	C1–N2–C3	134 (2)
C1–Ir2–C211	102.8 (5)	Ir1–C111–N112	176 (1)
C1–Ir2–C221	151.6 (6)	C111–N112–C113	176 (1)
C211–Ir2–C221	105.4 (6)	Ir1–C121–N122	175 (1)
Ir1–P11–C-B1	114.3 (5)	C121–N122–C123	168 (1)
Ir1–P11–C11-1	116.9 (6)	Ir2–C211–N212	177 (1)
Ir1–P11–C11-2	114.7 (5)	C211–N212–C213	179 (1)
C-B1–P11–C11-1	103.3 (6)	Ir2–C221–N222	172 (1)
C-B1–P11–C11-2	103.8 (6)	C221–N222–C223	176 (1)

[a] Numbers in parentheses are estimated standard deviations in the least significant digits.

Table IV. Rate Constants for the Hydrogenation of **1** to **2** at Various Temperatures[a]

T, K	*k*, s^{-1}	*T*, K	*k*, s^{-1}
273	2×10^{-6}	298	2×10^{-4}
286	4×10^{-5}	309	9×10^{-4}

[a] All kinetic studies were done in THF solution. Activation parameters were calculated from $\ln (k/T) = [(\Delta S^*/R) - \ln (h/k')] - (\Delta H^*/RT)$, $\Delta H^* = 28$ kcal mol^{-1}, and $\Delta S^* = 18$ cal mol^{-1} K^{-1}.

singlet for the xylyl isocyanides observed at δ 2.43 at room temperature emerged as three distinct peaks of relative intensities 2:2:1 at −80 °C (Figure 2). These are assigned to the methyl protons of the two types of terminal and one type of bridging xylyl isocyanide ligands. From the coalescence temperature of −26 °C, we have calculated $k = 45$ s^{-1} and $\Delta G^* = 12.5 \pm 0.3$ kcal mol^{-1}. An interesting question pertaining to the independently observed dmpm methyl and bridge–terminal isocyanide exchange is whether or not they occur via the same process.

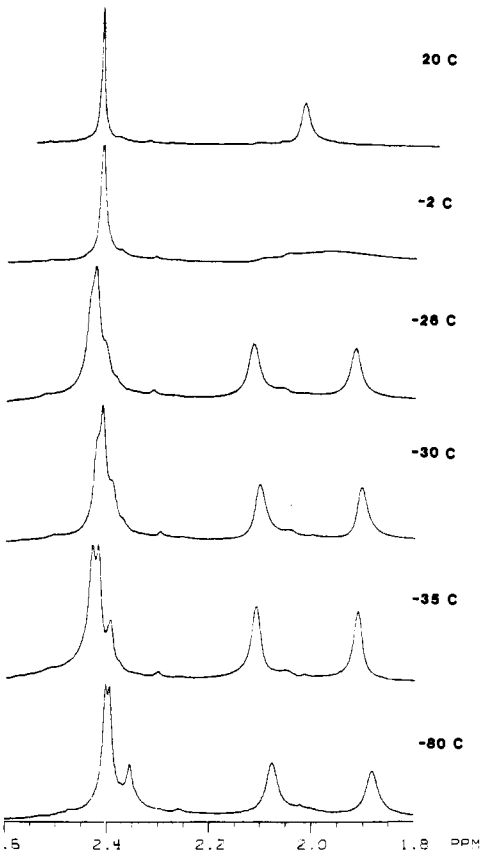

Figure 2. Variable-temperature 470-MHz ^1H NMR spectrum of $[Ir_2(\mu\text{-CNR})(CNR)_4(dmpm)_2][PF_6]_2$ (**1**) in CD_2Cl_2 solution. Below −2 °C, two distinct dmpm methyl environments are evident at 1.92 and 2.12 ppm. At lower temperatures three distinct 2,6-xylyl isocyanide methyl environments are evident at 2.35–2.45 ppm.

A direct comparison of the rates of exchange of the dmpm vs. the xylyl isocyanide methyl environments was possible when the variable low-temperature ^1H NMR experiments was performed by using a 200-MHz instrument. The methyl protons of the dmpm ligands coalesced at −20 °C, with the following apparent rate constant and activation energy at −26 °C: $k = 50$ s^{-1} and $\Delta G^* = 12.5 \pm 0.5$ kcal mol^{-1}. These compare well with those values obtained for the exchange of the xylyl isocyanide ligands at the same temperature in the 470-MHz study. The similarity of rates and activation energies clearly favor a common mechanism for both observed exchanges. We note the dmpm methyl environments can easily be equilibrated in principle by isocyanide bridge $\rightleftarrows$ terminal exchange, but no dynamic process involving the dmpm ligands alone can equilibrate bridge and terminal isocyanide sites. Our results therefore imply that the dmpm methyl environments are rendered equivalent by rotation of the five isocyanide ligands about the $Ir_2(dmpm)_2$ framework.

Hydrogenation of $[Ir_2(\mu\text{-CNR})(CNR)_4(dmpm)_2]^{2+}$ to $[Ir_2(H)_2(CNR)_4(dmpm)_2]^{2+}$ (R = 2,6-Me_2-C_6H_3, *t*-C_4H_9). Complexes **1** and **3** react efficiently with H_2. The reactions with H_2 result in displacement of one isocyanide to give the dihydrides $[Ir(H)_2(CNR)_4(dmpm)_2]^{2+}$ (R = 2,6-Me_2-C_6H_3 (**2**), *t*-C_4H_9 (**4**)). Dihydrides **2** and **4** are obtained as analytically pure, pale yellow solids. The IR spectra display only terminal ν(CN) bands at 2146 (s), 2127 (s), and 1995 (w) cm^{-1} for **2**, and at 2168 (s), 2147 (s), and 2051 (w) cm^{-1} for **4**. The hydride ^1H NMR signals for **2** and **4** both appear as symmetric phosphorus split quintets. The symmetric nature of these complexes is evident in results of selectively proton-decoupled ^{31}P NMR experiments. Figure 3a shows the fully proton-coupled ^{31}P NMR spectrum of **2**. When the spectrum of **2** is decoupled from all protons resonating at field strengths less than 0 ppm, the ^{31}P NMR spectrum shown in Figure 3b is observed. This spectrum results from coupling to the hydrides of **2** only and appears as a symmetric triplet. These results,

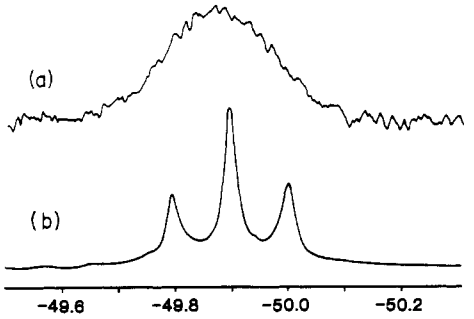

Figure 3. ^{31}P NMR spectrum of $[Ir_2(\mu\text{-}H)_2(CN\text{-}2,6\text{-}Me_2C_6H_3)_4(dmpm)_2][PF_6]_2$ (**2**): (a) coupled to all protons; (b) coupled to hydrides only.

together with the integration of the hydride resonance relative to the dmpm methyl and methylene resonances, suggest that there are two hydridic protons in a molecule of **2** and these protons are equivalent. The average symmetric $(\mu\text{-}H)_2$ structures of **2** and **4**, evident in the ^1H and $^{31}P\{$selective $^1H\}$ NMR spectra, are preserved at temperatures as low at −60 °C. We conclude that the symmetric structure II accurately depicts the average structures of **2** and **4** in solution.

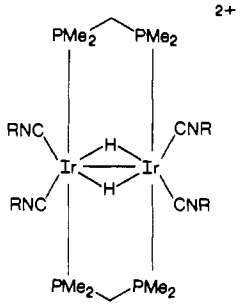

II (R=2,6-Me_2-C_6H_3 (**2**), t-C_4H_9 (**4**))

The reactions of **1** and **3** with H_2 can be viewed as substitutions of a bridging isocyanide ligand by dihydrogen. The course of these hydrogenations is conveniently monitored by IR in the C≡N stretching region (Figure 4). We have examined the kinetics of the binuclear complex reaction for the case of the 2,6-xylyl derivative, **1**. The overall reaction is given in eq 1. The addition

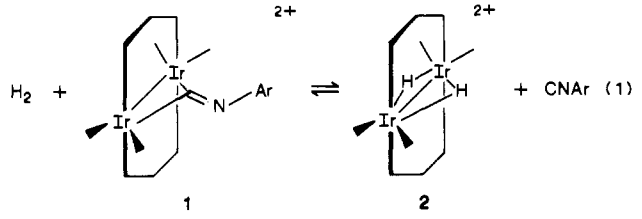

of H_2 to **1** was studied over the temperature range 0–36 °C in THF solution. Details of the kinetics studies are given in the Experimental Section. The reaction is first order in [**1**] and zero order in $[H_2]$. First-order rate constants of the reaction, eq 1, are given in Table IV. The activation parameters for the addition of H_2 to **1** are $\Delta H^* = 28$ kcal mol^{-1} and $\Delta S^* = 18$ cal mol^{-1} K^{-1}. The substantial positive entropy of activation is unusual for an oxidative addition of H_2. There are relatively few systems for

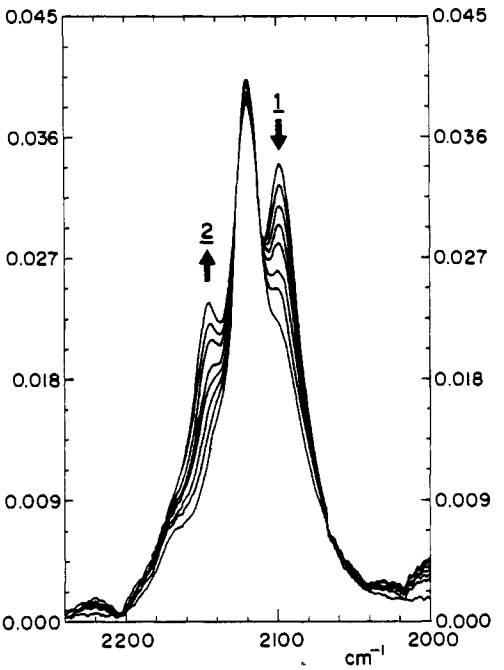

Figure 4. IR spectrum in the C≡N stretching region for the reaction of $[Ir_2(\mu\text{-}CN\text{-}2,6\text{-}Me_2C_6H_3)(CN\text{-}2,6\text{-}Me_2C_6H_3)_4(dmpm)_2][PF_6]_2$ (**1**) with H_2 to form $[Ir_2(\mu\text{-}H)_2(CN\text{-}2,6\text{-}Me_2C_6H_3)_4(dmpm)_2][PF_6]_2$ (**2**).

which the kinetics of ligand displacement by H_2 have been investigated, however. The zero-order dependence on $[H_2]$ and the positive entropy of activation are consistent with a dissociative mechanism. The rate-determining step for the reaction, eq 1, is very likely dissociation of CNAr. In accordance with the exchange of isocyanide ligands in solution, a possible mechanism is the loss of a terminal CNAr ligand, followed by exchange of an isocyanide from a bridging to a terminal position. In the subsequent steps, the diiridum intermediate rapidly reacts with 1 equiv of H_2 to give the dihydride complex **2**. Such a mechanism would accommodate the overall first-order nature of the H_2 addition and the substantial entropy of the activated complex.

Acknowledgment. This work was supported by the National Science Foundation through Grant CHE-8411836 and the Materials Research Laboratory at Purdue University. Additional support from Stauffer Chemical Co. is gratefully acknowledged. M.K.R. wishes to acknowledge a David Ross Fellowship. The assistance of Dr. Claude Jones in obtaining selectively proton-decoupled phosphorus NMR spectra is gratefully acknowledged. A generous loan of $IrCl_3$ from Johnson Matthey, Inc., is appreciated. NIH support, Grant RR-01077, of the Biochemical Magnetic Resonance Laboratory at Purdue is acknowledged. The PDP 11/34 computer and X-ray structure solution of the Department of Chemistry were purchased with funds from the NSF Chemical Instrumentation Program (Grant CHE-8204994) and the Monsanto Fund.

Supplementary Material Available: Tables of general temperature factor expressions, all bond distances and angles, least-squares planes, and dihedral angles (13 pages); a listing of observed and calculated structure factors (24 pages). Ordering information is given on any current masthead page.